Eur. Phys. J. Special Topics **222**, 1–8 (2013)

DOI: 10.1140/epjst/e2013-02023-x

THE EUROPEAN PHYSICAL JOURNAL SPECIAL TOPICS

Regular Article

Generators of quasiperiodic oscillations with three-dimensional phase space

A.P. Kuznetsov[1], S.P. Kuznetsov[1], E. Mosekilde[2,a], and N.V. Stankevich[3,b]

[1] Saratov Branch of Institute of Radio-Engineering and Electronics of RAS, 410019, Russia, Saratov, Zelenaya, 38
[2] Department of Physics, The Technical University of Denmark, DK-2800 Kgs. Lyngby, Denmark
[3] Saratov State Technical University, 410054, Russia, Saratov, Polytechnicheskaya, 77

Received 16 July 2013 / Received in final form 13 August 2013
Published online xx September 2013

Abstract. Considering a family of three-dimensional oscillators originating in the field of radio-engineering, the paper describes three different mechanisms of torus formation. Particular emphasis is paid to a process in which a saddle-node bifurcation eliminates a stable cycle and leaves the system to find a stationary state between a saddle cycle and a pair of equilibrium points of unstable focus/stable node and unstable node/stable focus type.

1 Introduction

Quasiperiodicity is a form of behavior that can be observed in nonlinear dynamic systems from almost all areas of science and technology [1]. It is also known that this form of behavior plays a significant role in connection with a broad range of important phenomena, including synchronization [2], torus breakdown [3], the transition to turbulence [4], and the role of KAM-tori in conservative systems [5].

In general terms, quasiperiodicity may be thought of as a form of dynamics that consists of two (or more) oscillatory components with incommensurate frequencies. Classical conceptions of the onset of turbulence (Landau theory, 1944), for instance, involved an infinite cascade of Hopf bifurcations, producing quasiperiodic states of continuously increasing dimension. During the 1970's, a series of experiments on the onset of turbulence in simple geometries failed to support this picture [6]. The experiments showed power spectra characteristic of a first and a second Hopf bifurcation. However, rather than the peaks associated with a third Hopf bifurcation, a strong noisy background appeared. At the same time, a remarkable theorem by Newhouse et al. [7,8] showed that a state of three-dimensional quasiperiodicity is unstable to small perturbations, suggesting that quasiperiodicity of dimension three or more is unlikely to be observed in nature.

[a] e-mail: erik.mosekilde@fysik.dtu.dk
[b] e-mail: stankevichnv@mail.ru

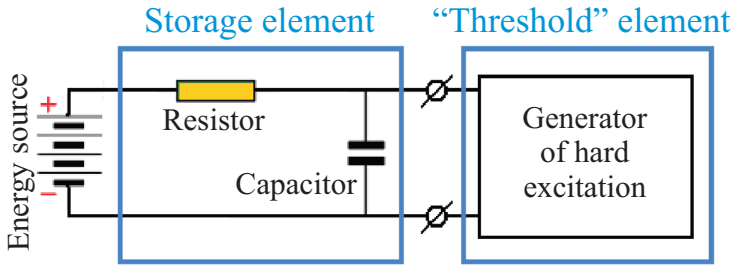

Fig. 1. (Color online) Generator circuit.

In spite of these findings, examples of persistent three-dimensional quasiperiodicity in computer simulations are easy to find in the literature [9–12] and this line of research continues to be actively pursued, for instance, through the study of so-called phase synchronized quasiperiodicity [13,14].

The complementary situation of quasiperiodicity in systems with very low dimensional phase spaces has attracted considerable less attention. Anishchenko et al. [15,16] have proposed a new autonomous system of dimension four and have demonstrated both the appearance of two-frequency dynamics and a sequence of period-doubling bifurcations of the two-dimensional torus. In particular, these authors have observed that resonance phenomena do not occur near the points of torus doubling.

Quasiperiodicity is also known to occur in autonomous systems with a phase space dimension of only three. Particularly interesting in this connection is the demonstration by Genesio and Ghilardi [17] that several of the well-known chaos-generating oscillators, e.g., both the Rössler and the Chua systems, generate stable quasiperiodicity in certain parameter regions. Quasiperiodicity is also known to arise in systems of two coupled nearly identical period-doubling oscillators [1], [18]. Here one observes that the first period-doubling bifurcation in the case of dissipative coupling is replaced by a torus bifurcation.

The purpose of the present paper is to extend recent work on torus formation mechanisms in low-dimensional systems initiated by Kuznetsov et al. [19]. We consider a family of three-dimensional systems derived from the field of radio-engineering. Particular emphasis is given to the formation of a torus through a saddle-node bifurcation that eliminates the only stable cycle in the system and leaves the dynamics to settle down in the presence of a limit cycle (S_1) of saddle type and of a pair of equilibrium points (E_1 and E_2) of unstable focus/stable node and of stable focus/unstable node type.

2 Three-dimensional generator of quasiperiodic oscillations: Principle of operation

The starting point for the present analysis is the three-dimensional oscillator system

$$\ddot{x} - (\lambda + z + x^2 - \beta x^4)\dot{x} + \omega_0^2 x = 0, \dot{z} = \mu - x^2 \tag{1}$$

recently proposed by Kuznetsov et al. [19]. These equations represent an example of a minimal system that can exhibit quasiperiodic dynamics. At the same time the equations are related to formulations that have been used to produce structurally stable chaos [20,21].

As illustrated in Fig. 1, the two equations of motion can be thought of as describing a storage element coupled to a threshold element in the form of a generator of

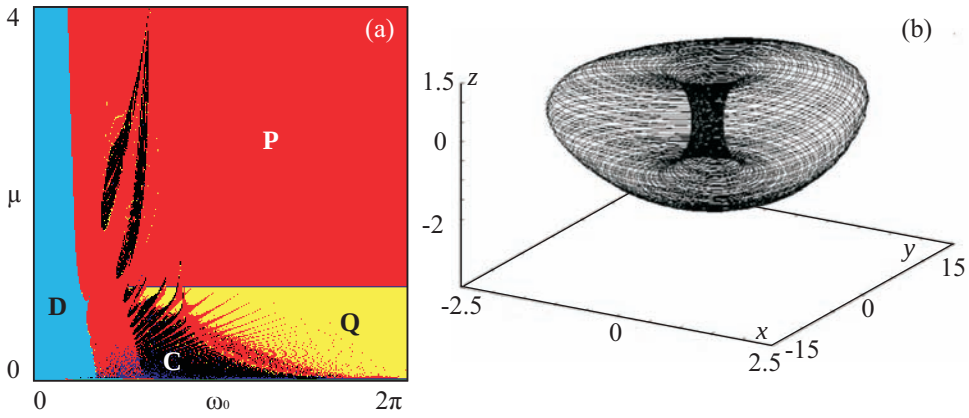

Fig. 2. (Color online) (a) Chart of dynamical modes in the (ω_0, μ) parameter plane. $\lambda = 0$ and $\beta = 0.5$. (b) Three-dimensional phase portrait of the quasiperiodic attractor that exists in our coupled oscillator system for $\lambda = 0$, $\beta = 0.5$, $\mu = 0.9$, and $\omega_0 = 2\pi$. The variable y represents $\dot{x}$. Main regimes on the charts of dynamical modes were denoted by corresponding palette and letters: **E** - stable equilibrium point (white); **P** - periodic regimes [red (dark grey)]; **Q** - quasiperiodic regimes [yellow (light grey)]; **C**- chaotic regimes (black); **D** - regime of divergency [blue (grey)].

hard oscillations. The first equation in Eq. (1) describes the threshold element. The subcritical nature of the Hopf bifurcation produced by this element sets the thresholds for different forms of behavior and also introduces hysteresis (memory) into the system. The degree of subcriticality is controlled by the parameter β. The second equation in Eq. (1) describes the storage element as a capacitor that is continuously charged at a rate μ and discharged at a rate proportional to the intensity x^2 of the oscillations generated by the threshold element. At the same time, the term z in the equation for the threshold element introduces a modulation of the rate of growth of the oscillations in this element that depends of the charging state of the storage element. For $\lambda = 0$, the temporal behavior of the coupled oscillator system may be described in terms of the following sequence of four phases that continuously repeats itself: (**A**) Starting in a situation where the storage variable z is negative and close to its minimum, the self-oscillator operates in a regime of stable equilibrium dynamics. Existing oscillations in x gradually decrease, and recharging of the storage element occurs at increasing speed. (**B**) When z becomes positive, the self-oscillator undergoes a subcritical Hopf bifurcation and, seeded by the remaining small amplitude oscillations, the amplitude of the oscillations in the threshold element increases quickly. (**C**) As the amplitude of the self-oscillations become larger, discharging of the storage element starts to occur more rapidly, and z begins to decrease. (**D**) Due to the subcritical nature of the Hopf bifurcation, the amplitude of the x-oscillations remains large, until z becomes negative. The x-oscillations then again start to decrease in amplitude, leading to a slower discharging rate for the storage element. The parameters ω_0 and μ control the frequencies of oscillation and modulation, respectively, and with appropriate parameter values the system will display quasiperiodicity.

Figure 2(a) presents a chart of dynamical modes for the parameter plane scanned by the basic operational frequency ω_0 for the self-oscillator and the basic charging rate μ for the storage system. Here, **P** [red (dark grey)] denotes regimes of periodic solutions, **Q** [yellow (light grey)] regimes of quasiperiodic solutions, **C** (black) regimes of chaotic solutions, and **D** [blue (grey)] a regime of divergence. Following Poliashenko et al. [22], construction of the chart in Fig. 2(a) was based on a calculation of the three Lyapunov exponents for the coupled oscillator system. The chaotic regime to

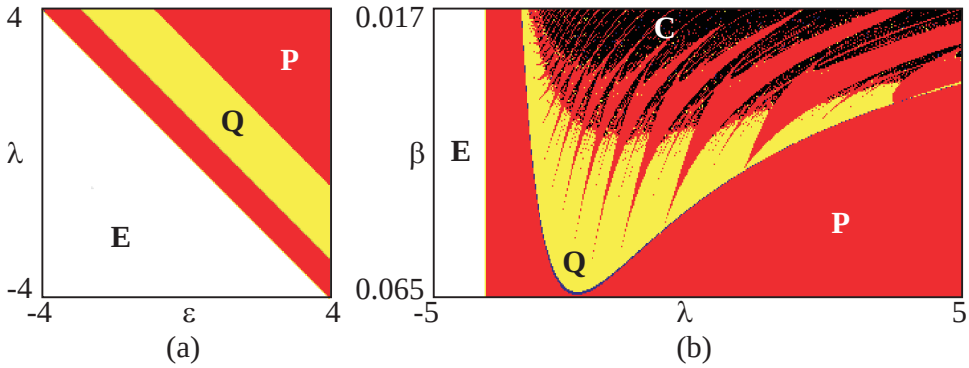

Fig. 3. (Color online) Chart of dynamical modes in the system described by Eq. 2. (a) Transitions from the stable equilibrium point **E** to periodic dynamics **P** and quasiperiodicity **Q** in the (ε, λ) parameter plane. $k = 0.02$, $\beta = 0.056$, and $\omega_0 = 2\pi$. (b) Synchronization tongues and transitions to chaos in the (λ, β) parameter plane. $\varepsilon = 4$, $k = 0.02$, $b = 1$, and $\omega_0 = 2\pi$.

the upper left in the main region of periodic dynamics is reached from both sides through a cascade of period-doubling bifurcations. The straight line between periodic and quasiperiodic dynamics for $\mu = 1$ represents a secondary Hopf (or torus-birth) bifurcation. It should also be noted that parts of the diagram involve coexisting solutions. Figure 2(b) shows a phase portrait of the quasiperiodic oscillator that exists for $\lambda = 0$, $\beta = 0.5$, $\mu = 0.9$, and $\omega_0 = 2\pi$. In this figure, the variable y denotes $\dot{x}$.

3 Low-dimensional quasiperiodicity from a single equilibrium point

It is interesting to note that the coupled oscillator system considered in Sect. 2 did not exhibit any form of equilibrium. The simplest form of dynamics it can display is a periodic cycle. Hence, we cannot follow the emergence of the quasiperiodic attractor from an initially stable equilibrium point. This limitation may be ascribed to the formulation of the charging relation in Eq. (1). Actually, with a fixed external charging rate of μ, this equation represents a constant current source rather than the constant voltage source shown in Fig. 1. To take hand of this problem one can reformulate the charging equation to read

$$\ddot{x} - (\lambda + z + x^2 - \beta x^4)\dot{x} + \omega_0^2 x = 0, \dot{z} = b(\varepsilon - z) - k\dot{x}^2, \tag{2}$$

where the parameters ε and b can be interpreted as the voltage of the charging battery and the conductance of the series resistor, respectively. The form of the discharging rate is maintained with the exception that a scaling factor k has been introduced. This parameter will typically take values of $k = 0.02$.

With this reformulation, our coupled oscillator system now has a single equilibrium point in (x,$\dot{x}$,z) = (0, 0, ε). When the system is linearized around this point, the x- and z-dynamics separate, and we immediately find the eigenvalues $L_1 = -b$ for the z-direction and $L_{2,3} = \frac{1}{2}[\lambda + \varepsilon \pm \sqrt{(\lambda + \varepsilon)^2 - 4\omega_0^2}]$ for the (x, $\dot{x}$) plane. As long as b is positive the equilibrium point will be stable in the z-direction. However, the equilibrium point will display a Hopf bifurcation in the xy-plane for $\lambda + \varepsilon = 0$.

Figure 3(a) illustrates the observed bifurcation structure. The region where a stable equilibrium point exists is denoted **E** and shown in white. As before, periodic

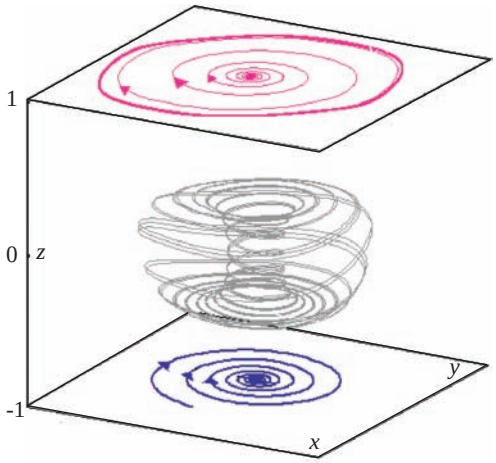

Fig. 4. (Color online) Structure of the phase space for the system with limited net charging rate. The upper equilibrium point is a stable node in the z-direction and an unstable focus point in the transverse plane. The lower equilibrium point is repelling in the z-direction and a stable focus in the transverse directions. Note the two-dimensional torus that exists between the two planes. $\lambda = 0$, $\beta = 0.5$, $c = 1$, $\mu = 0.9$, and $\omega_0 = 2\pi$.

regimes are colored red (dark grey) and denoted by a **P** while the regime of quasi-periodicity is denoted **Q** and colored yellow (light grey). The mode distribution was again determined by calculation of the three Lyapunov exponents. Figure 3(b) shows the distribution of dynamic modes in the (λ, β) parameter plane. This figure illustrates the transition to quasiperiodicity, the appearance of resonance tongues, and the final development of chaotic dynamics through torus breakdown as the parameter β that controls the subcriticallity of the Hopf bifurcation in the x-dynamics becomes sufficiently small.

4 Torus birth process involving two distinct equilibrium points

Aside from the fact that the torus formation process took place in a low-dimensional phase space and involved a subcritical Hopf bifurcation in the threshold element, the transition described in Sect. 3 represents a classical torus birth process as it proceeds through first a Hopf bifurcation and thereafter a secondary Hopf bifurcation.

An alternative modification of the original charging equation could take the form

$$\ddot{x} - (\lambda + z + x^2 - \beta x^4)\dot{x} + \omega_0^2 x = 0, \quad \dot{z} = (\mu - x^2)(c^2 - z^2). \tag{3}$$

This formulation still allows us to consider the charging process to take place from a constant current source. However, the net charging rate is now regulated by a limiting mechanism that protects the system from reaching rates outside of the interval $[-c,c]$.

The coupled oscillator system now displays two different equilibrium points $(x,\dot{x},z) = (0,0,\pm c)$. Calculation of the eigenvalues for these equilibrium points gives $L_1 = \mp 2\mu c$, $L_{2,3} = \frac{1}{2}[(\lambda \pm c) \pm \sqrt{(\lambda \pm c)^2 - 4\omega_0^2}]$, and the conditions for Hopf bifurcations of the two equilibrium points are $\lambda \pm c = 0$, respectively. For positive values of c, the equilibrium point at $z = c$ is attracting in the z-direction and an unstable focus point in the transverse directions. With the same condition, the equilibrium point at $z = -c$ is repelling in the z-direction and an attracting focus point in the transverse directions.

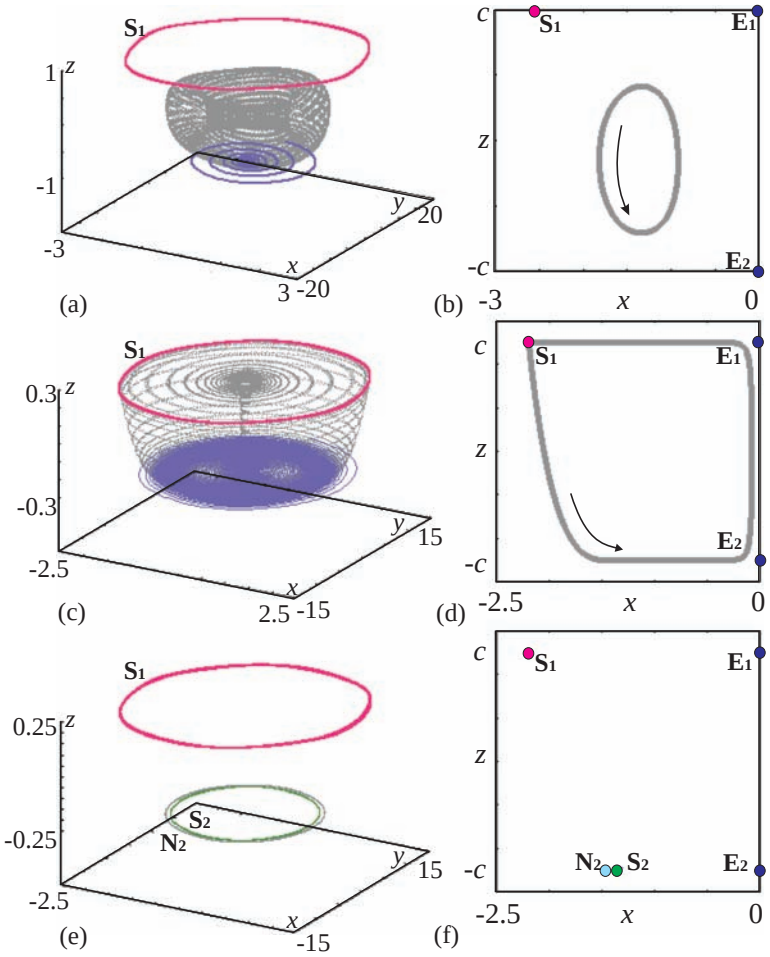

Fig. 5. (Color online) Torus destruction as the distance between the two planes in Fig. 4 is reduced. (a) Fully developed torus with its cross section (b). $c = 1$ (c) The torus is squeezed between the two planes and finally collides simultaneously with the two equilibrium points E_1 and E_2 and with the saddle cycle S_1. (d) Torus cross section immediately before the destruction. $c = 0.249$ (e) The torus destruction process is accompanied by the appearance of the pair of saddle and stable node cycles S_2 and N_2. $c = 0.251$. $\beta = 0.5$.

An interesting aspect of the modified structure is that it allows a two-dimensional torus to exist between the planes $z = \pm c$. This is illustrated in Fig. 4 for $\lambda = 0$, $\beta = 0.5$, $c = 1$, $\mu = 0.9$, and $\omega_0 = 2\pi$. Inspection of the figure shows how the stationary trajectory on the torus spirals upwards with a relatively small amplitude in its horizontal dynamics and how this amplitude gradually increases as the trajectory approaches the upper plane with its expanding focus dynamics.

However, while the equilibrium point in the upper plane is attracting in the z-direction, the associated limit cycle is unstable in this direction. As a result, the trajectory turns around and starts to spiral downwards. In the beginning, the oscillator amplitude still increases. However, as the trajectory approaches the lower plane with its stable focus point, the amplitude in the horizontal oscillations again decreases. Finally, as the trajectory comes close to the focus point in the lower plane, which is repelling in the z-direction, the trajectory starts to spiral upwards anew.

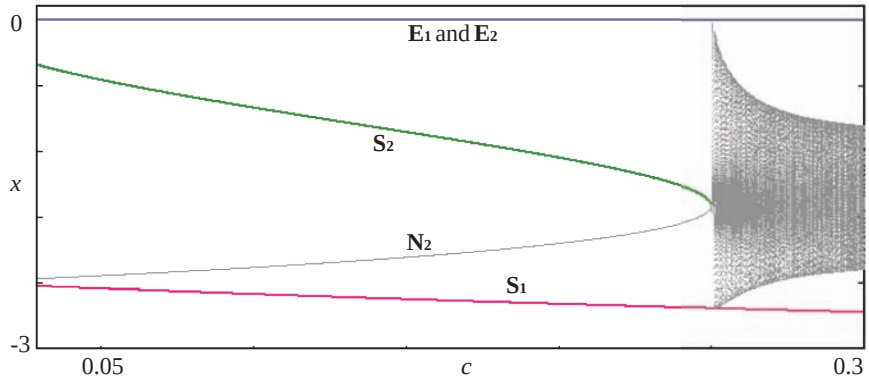

Fig. 6. (Color online) Bifurcation diagram for the torus destruction/torus birth process illustrated in Fig. 5. The horizontal line represents the two equilibrium points at $x = 0$, $z = \pm c$, and S_1 are the saddle cycle that coexists with the fully developed torus. N_2 and S_2 is a node and a saddle cycle that exist in the lower plane ($z = -c$) for small values of c.

5 Scenario of torus birth/destruction for oscillator system with two equilibrium points

The main dynamics associated with the fully developed torus discussed in Sect. 4 is repeated in Fig. 5(a) Here, we see the torus itself, the stable limit cycle in the upper plane $z = c$, and the spiralling approach to the stable focus point in the lower plane $z = -c$. Figure 5(b) shows a crossection of the torus and the associated structures. In this figure, S_1 represents the limit cycle in the upper plane, while E_1 and E_2 represent the equilibrium points in the lower and upper planes.

As the distance between the two planes is reduced, the space available for the two-dimensional torus becomes more and more restricted, and the torus is forced to approach both the limit cycle in the upper plane and the two equilibrium points. This is illustrated in Figs. 5 (c) and (d).

Finally, as the lower plane with decreasing values of c is shifted into the regime of subcritical dynamics for the threshold oscillator, a pair of stable and unstable limit cycles are formed in this plane around the unstable focus point. The presence of these limit cycles distorts the flow and, as illustrated in Fig. 5(e), the torus disappears. In Fig. 5(f), the two new limit cycles are represented by a light blue and a green dot for the stable and the saddle cycle, N_2 and S_2 respectively. If the same process is followed in the opposite direction (i.e., for increasing values of c), one can observe the birth of the torus as the lower plane ($z = -c$) moves out of the regime of co-existing stable and unstable limit cycles for the threshold oscillator. This is illustrated in Fig. 6.

6 Conclusion

The aim of the present study has been to investigate torus formation in systems with three dimensional phase spaces. Using concepts from radio-engineering we have examined three different versions of a coupled oscillator system in which the charging and discharging dynamics of a relaxation oscillator enter into a feedback with a self-oscillator that displays a subcritical Hopf bifurcation. With this structure, the dynamics of the examined systems exhibit two characteristic time scales, a slow time scale associated with the charging dynamics and a faster time scale associated with

the self-oscillations. Other examples of the same general structure may be found in the interaction between the slow calcium dynamics and the faster potassium dynamics of bursting biological cells [23]. From a nonlinear dynamics point of view, the study has led us to consider torus formation in systems without equilibrium points as well as with one or two equilibrium points. A particular interesting phenomenon is the development of quasiperiodicity in systems where the steady state dynamics is contained by the invariant manifolds of two equilibrium points and a saddle cycle.

This research was supported, in part, by the grants of RFBR. A.P.K. and S.P.K. acknowledge partial support from the RFBR-DFG grant No 11-02-91334. N.V.S. acknowledges partial support from the RFBR grant No 12-02-31465. N.V.S. thanks the Danish Medicines Agency for supporting her visit to The Technical University of Denmark.

References

1. V.S. Anishchenko, *Dynamical Chaos in Physical Systems* (Teubner, Leipzig, 1985)
2. A. Balanov, N. Janson, D. Postnov, O. Sosnovtseva, *Synchronization: From Simple to Complex* (Springer, Berlin, 2009)
3. I.A. Kuznetsov, *Elements of Applied Bifurcation Theory* (Springer, New York, 2004)
4. G.I. Barenblatt, G. Iooss, D.D. Joseph, *Nonlinear Dynamics and Turbulence* (Pitman Publ., London, 1983)
5. J. Moser, *Stable and Random Motion in Dynamical Systems* (Princeton University Press, 1973)
6. P.R. Fenstermacher, H.L. Swinney, J.P. Gollub, J. Fluid Mech. **94**, 103 (1979)
7. D. Ruelle, F. Takens, Commun. Math. Phys. **20**, 167 (1971)
8. S.E. Newhouse, D. Ruelle, F. Takens, Commun. Math. Phys. **64**, 33 (1978)
9. R.K. Tavalkov, A.S. Tworkowski, Phys. Lett. A **100**, 65 (1984)
10. P.M. Battelino, Phys. Rev. E **38**, 1495 (1988)
11. P. Linsay, A. Cummings, Physica D, **40**, 196 (1989)
12. U. Feudel, W. Jansen, J. Kurths, Int. J. Bifurc. Chaos, **3**, 131 (1993)
13. V. Anishchenko, M. Safonova, U. Feudel, J. Kurths, Int. J. Bifurc. Chaos, **4**, 595 (1994)
14. J.L. Laugesen, E. Mosekilde, N.-H. Holstein-Rathlou, Chaos, **21**, 033128 (2011)
15. V.S. Anishchenko, S.M. Nikolaev, Tech. Phys. Lett. **31**, 853 (2005)
16. V.S. Anishchenko, S.M. Nikolaev J. Kurths, Phys. Rev. E, **73**, 056202 (2006)
17. R. Genesio, C. Ghilardi, Int. J. Bifurc. Chaos, **15**, 3165 (2005)
18. C. Reick, E. Mosekilde, Phys. Rev. E,**52**, 1418 (1995)
19. A.P. Kuznetsov, S.P. Kuznetsov, N.V. Stankevich, Commun. Nonl. Sci. Num. Sim. **15**, 1676 (2010)
20. S.P. Kuznetsov, *Hyperbolic chaos: A Physicist's view* (Higher Education Press: Beijing and Springer: Heidelberg, 2011)
21. S.P. Kuznetsov, A. Pikovsky, Physica D, **232**, 87 (2007)
22. M. Poliashenko, S.R. McKay, C.W. Smith, Phys. Rev. A, **44**, 3452 (1991)
23. E.M. Izhikevich, Int. J. Bif. Chaos, **10**, 1171 (2000)